

See discussions, stats, and author profiles for this publication at: <https://www.researchgate.net/publication/51875393>

Selection and Characterization of PCB-Binding DNA Aptamers

ARTICLE in ANALYTICAL CHEMISTRY · DECEMBER 2011

Impact Factor: 5.64 · DOI: 10.1021/ac202960b · Source: PubMed

CITATIONS

18

READS

84

9 AUTHORS, INCLUDING:



[Elsa Rouah](#)

University of Antwerp

15 PUBLICATIONS 182 CITATIONS

[SEE PROFILE](#)



[Marie-Louise Scippo](#)

University of Liège

116 PUBLICATIONS 1,897 CITATIONS

[SEE PROFILE](#)



[Freddy Dardenne](#)

University of Antwerp

20 PUBLICATIONS 172 CITATIONS

[SEE PROFILE](#)



[Johan Robbens](#)

Institute for Agricultural and Fisheries Research

82 PUBLICATIONS 1,098 CITATIONS

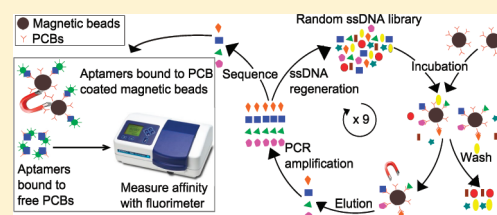
[SEE PROFILE](#)

Selection and Characterization of PCB-Binding DNA Aptamers

Jaytry Mehta,^{*,†,‡} Elsa Rouah-Martin,^{†,‡} Bieke Van Dorst,^{†,‡,#} Bert Maes,[§] Wouter Herrebout,[§] Marie-Louise Scippo,[⊥] Freddy Dardenne,[†] Ronny Blust,[†] and Johan Robbins^{†,‡}Laboratory for Ecophysiology, Biochemistry and Toxicology, [†]Department of Biology, University of Antwerp, Groenenborgerlaan 171, B-2020 Antwerp, Belgium[‡]Institute for Agricultural and Fisheries Research, Ankerstraat 1, B-8400, Oostende, Belgium[§]Department of Chemistry, University of Antwerp, Groenenborgerlaan 171, B-2020 Antwerp, Belgium[⊥]Food Sciences Department, University of Liège, Boulevard de Colonster, 20, B-4000 Liège, Belgium

S Supporting Information

ABSTRACT: Polychlorinated biphenyls (PCBs) are persistent organic pollutants (POPs) that resist natural degradation and bioaccumulate in nature. Combined with their toxicity, this leads them to cause cancer and other health hazards. Thus, there is a vital need for rapid and sensitive methods to detect PCB residues in food and in the environment. In this study, PCB-binding DNA aptamers were developed using PCB72 and PCB106 as targets for aptamer selection. Aptamers are synthetic DNA recognition elements which form unique conformations that enable them to bind specifically to their targets. Using in vitro selection techniques and fluorometry, an aptamer that binds with nanomolar affinity to both the PCBs has been developed. It displayed high selectivity to the original target congeners and limited affinity toward other PCB congeners (105, 118, 153, and 169), suggesting general specificity for the basic PCB skeleton with varying affinities for different congeners. This aptamer provides a basis for constructing an affordable, sensitive, and high-throughput assay for the detection of PCBs in food and environmental samples and offers a promising alternative to existing methods of PCB quantitation. This study therefore advances aptamer technology by targeting one of the highly sought-after POPs, for the first time ever recorded.



Polychlorinated biphenyls (PCBs) are a group of 209 individual congeners that belong to a broad family of man-made organic chemicals known as chlorinated hydrocarbons. They were widely used as lubricants and coolants in a variety of industrial and electrical applications, because of their nonflammability, chemical stability, high boiling point, and electrical insulating properties.¹ However, these very characteristics make them resistant to natural degradation and persistent in the environment,² and therefore they have been classified as persistent organic pollutants (POPs), along with several other compounds.³ Their natural propensity to bioaccumulate and biomagnify, combined with their toxicity, leads them to cause cancer⁴ and other adverse health effects on the immune system, reproductive system, nervous system, and endocrine system.⁵ Even though production was banned more than two decades ago in several countries (76/403/EEC which refers to the directive of the council of the European community), trace levels of PCBs are still present in the environment, continuing to pose a major threat to public health.⁶ The possible sources of exposure to these ubiquitous environmental pollutants include consuming food and water containing PCBs, breathing air with PCBs, and occupational health exposures.⁷ However, the most common source of exposure is from eating PCB-contaminated foods such as fish, eggs, red meat, poultry, milk, and cheese.⁸ The Food and Drug Administration (FDA) has designated tolerance levels for PCBs that range between 0.2 and 3 ppm in

food, and these residue limits are used to determine whether or not a food is safe to consume. Sensitive and cost-effective monitoring systems that enable rapid screening for PCBs in food and environmental samples are urgently needed to ensure food safety and to minimize risks for human and environmental health.

Currently, suspicious samples are routinely tested by gas chromatography–mass spectrometry (GC-MS) methods which are sensitive techniques⁹ but have some limitations such as the extensive costs incurred from sophisticated equipment and highly trained personnel. The conventional biosensors, which use enzymes or antibodies as recognition elements,¹⁰ are more cost-effective but lag in terms of stability and production time. Moreover, antibodies are obtained by immunizing animals and therefore, besides raising ethical concerns, they also cannot always be generated for small toxic agents or nonimmunogenic analytes. The limitations of these existing techniques have therefore propelled considerable research efforts toward the advancement of rapid, accurate, and economic alternative recognition elements. Aptamers, which are nucleic acid ligands, fulfill the current research requirements for affinity molecules and have therefore surfaced as promising alternatives. This class

Received: November 8, 2011

Accepted: December 14, 2011

Published: December 14, 2011

of recognition elements have even been termed as ‘chemical antibodies’¹¹ because of their unique conformations and detailed tridimensional structures that enable them to recognize a target, or a family of targets, very sensitively and selectively.¹² Moreover, the synthetic production of aptamers makes them animal-friendly and additionally enables them to be generated against toxic nonimmunogenic¹³ targets. They are also cost-effective, reproducible, and faster to produce than antibodies¹⁴ thereby offering an ethical alternative to the classic affinity molecules. It has been estimated that production costs of aptamers are 10–50 times lower than antibodies which necessitate in vivo production techniques.¹⁵ Added benefits of DNA aptamers include their ability to be functionalized, facilitating immobilization on sensor surfaces, and their superior stability, making them apt for measuring targets in complex matrices.

The applicability of DNA aptamers as recognition components in food and environmental biosensors has already been well-established for the detection of toxins such as 17 β -estradiol,¹⁶ oxytetracycline,¹⁷ botulinum neurotoxin,¹⁸ cholera toxin,¹⁹ ricin,²⁰ and ochratoxin A.²¹ Despite the huge potential of aptamers in general, to date no aptamers have been developed or even selected for any of the POPs, probably because of the nontriviality of fixing these stable unreactive chemical compounds onto solid supports. However, advancement in surface chemistry and collaboration between organic synthesis chemists and biotechnologists has recently opened avenues for the development of aptamers for more complex targets. Thereby, in this study, we present the first results of in vitro selections of novel single-stranded DNA aptamers that bind to PCBs with high molecular recognition. Specific aptamers that tightly bind PCBs were isolated from a random oligonucleotide library, by following an iterative selection procedure, known as Systematic Evolution of Ligands by EXponential enrichment (SELEX).²² This repetitive process consists of binding and elution steps of ligands in contact with the target molecule, until reaching an enriched pool of ligands containing high affinity for the target (Figure 1). The potential of aptamer technology is hereby further expanded by targeting a crucial class of POPs.

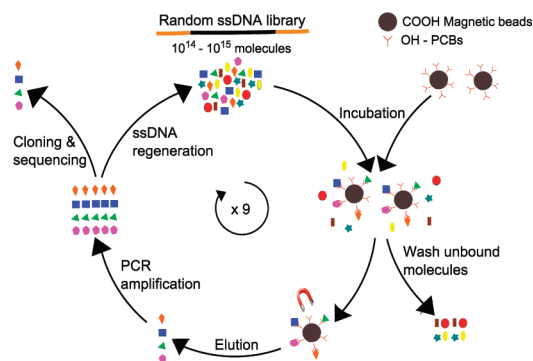


Figure 1. Aptamer selection procedure (SELEX).

EXPERIMENTAL SECTION

DNA Library and Primers. The random oligonucleotide library (5′-AGCAGCACAGAGGTCAGATG-N40-CCTATGCGTGCTACCGTGAA-3′) contained a central variable sequence of 40 nucleotides (N40) flanked by 20-nucleotide constant regions.²³ The following primers that

anneal to the 5′ and 3′ ends of the library were used for amplification of the selected oligonucleotides during the SELEX procedure: forward: 5′-AGCAGCACAGAGGTCAGATG-3′ and reverse: 5′-TTCACGGTAGCACGCATAGG-3′. Biotin-labeled 5′ reverse primer was used in polymerase chain reactions (PCR) for synthesizing biotin-labeled double-stranded DNA (dsDNA) products which were strand separated using streptavidin beads. The library and primers were chemically synthesized and high-performance liquid chromatography (HPLC) purified by Eurogentec (Belgium). They were dissolved in Milli-Q water (Millipore, Belgium) to get suitable template concentrations and kept at −20 °C until use.

Immobilization of PCBs onto Magnetic Beads. Carboxylic acid (COOH) Dynabeads MyOne (Invitrogen, Belgium) were used as immobilization matrices for the PCB targets. For the immobilization process, 4-hydroxy-2,3,5,5′-tetrachlorobiphenyl (OH-PCB72) and 2-hydroxy-2′,3′,4′,5′,5′-pentachlorobiphenyl (OH-PCB106) obtained from Accustandard (Da Vinci Europe Laboratory Solutions, Netherlands) were used. They have a functionalized OH group which makes them reactive for coupling onto COOH beads (Figure 2, parts

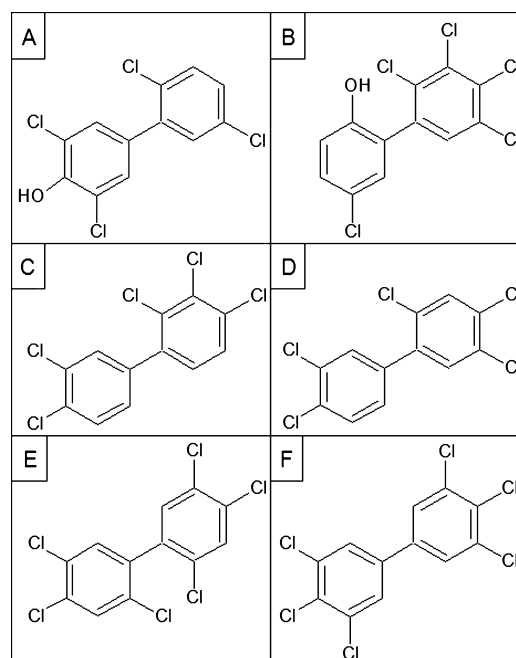


Figure 2. Chemical structures of (A) 4-hydroxy-2,3,5,5′-tetrachlorobiphenyl (OH-PCB72); (B) 2-hydroxy-2′,3′,4′,5′,5′-pentachlorobiphenyl (OH-PCB106); (C) PCB105; (D) PCB118; (E) PCB153; (F) PCB169.

A and B). Briefly, the procedure of coupling was as follows. The magnetic beads (2.5 mg) were washed and resuspended in 2.5 mL of dimethylformamide (DMF). An excess of OH-PCB (10 mg) and dicyclohexylcarbodiimide (DCC) (0.5 mg) was added to the beads solution and allowed to stir at 37 °C for 24 h, for binding to occur. The unreacted COOH groups on the beads were then quenched with 2.5 mL of a 50 mM ethanolamine solution (in DMF) by stirring at room temperature for 45 min. Finally, both sets of beads were each washed three times, resuspended in DMF, and stored at 4 °C until use. A separate aliquot of magnetic beads, coated only with ethanolamine, was also prepared for counter-selection purposes.

The coupling reactions of the two PCBs were confirmed using infrared (IR) spectroscopy by obtaining spectra of the targets themselves, the target-coated beads and the ethanolamine-coated beads, using an attenuated total reflection–Fourier transform (ATR-FT) IR spectrometer (Vector 22, Bruker). The IR spectra were recorded at a resolution of 4 cm^{-1} and were averaged over 100 scans.

In Vitro Selection of Aptamers for PCB72 and PCB106.

Aptamers with affinity for PCB72 and PCB106 were selected via an affinity selection procedure as illustrated in Figure 1. For the initial round of SELEX for each of the two PCBs, $72\text{ }\mu\text{g}$ of DNA library was added to $400\text{ }\mu\text{L}$ of binding buffer (BB) (100 mM NaCl , 20 mM Tris-HCl , 2 mM MgCl_2 , 5 mM KCl , 1 mM CaCl_2 , pH 7.6). Prior to its use in the binding reaction, the library was unfolded in BB at $90\text{ }^\circ\text{C}$ for 10 min and instantly cooled at $4\text{ }^\circ\text{C}$ for 15 min, followed by a 5-min incubation at room temperature (RT). In order to increase the specificity of the selected oligonucleotides, a counter-selection was performed before every round to facilitate elimination of nonspecific binding ssDNA with affinity for the background. For the counter-selection step, plain COOH-conjugated magnetic beads quenched with ethanolamine were used. The prepared ssDNA binding solution was preincubated with the ethanolamine quenched beads (2.7×10^8) on a rotary shaker for 30 min at RT. After 0.5 h, the ethanolamine-coated beads were pulled to a side of the tube using a magnet and the unbound aptamers in the supernatants were consequently transferred to PCB-coated magnetic beads in order to proceed with the target-binding selection step. For each SELEX round for each of the PCBs, 2.7×10^8 of the respective PCB-coated beads were used. Before each round, the beads were washed eight times in BB. After the last wash, the beads were resuspended in $100\text{ }\mu\text{L}$ of BB. The washed PCB-coated beads ($100\text{ }\mu\text{L}$) were then incubated with the ssDNA solution ($400\text{ }\mu\text{L}$) containing the unbound aptamers from the counter selection, for 30 min at RT, while tilting and rotating. Next, the unbound oligonucleotides were discarded by three washing steps using $500\text{ }\mu\text{L}$ of BB each time. Following the final wash, the bound oligonucleotides were eluted from the PCB-coated beads, by incubating the target–DNA complex twice in $200\text{ }\mu\text{L}$ of BB at $95\text{ }^\circ\text{C}$ for 9 min with gentle shaking and twice in $200\text{ }\mu\text{L}$ of elution buffer (EB) (40 mM Tris-HCl , 10 mM EDTA , 3.5 M urea , 0.02% Tween 20, pH 8.0) at $80\text{ }^\circ\text{C}$ for 7 min with gentle shaking, followed by magnetic separation of beads and ssDNA recovery. This process was repeated four times in order to recover all traces of bound DNA. The rest of the SELEX procedure (ethanol precipitation of the pooled eluted oligonucleotides, PCR, ssDNA preparation, cloning, and sequencing) was performed exactly as described previously.²⁴

In the ninth SELEX cycle, the ssDNA pool of the eighth round of selection using the OH-PCB72-coated beads was incubated with the OH-PCB106-coated beads and vice versa, in order to isolate common aptamers that could recognize both the target PCBs.

Sequence Analysis. The recovered sequences from the ninth SELEX round of both PCBs were aligned using GENEDOC software. Prediction of the lowest free-energy shapes and secondary structure analyses of the sequences were executed by using the free-energy minimization Zuker²⁵ algorithm via the Internet tool *mfold*.

Saturation Binding Assays and Dissociation Constant (K_d) Measurements. The binding kinetics of individual aptamers to PCB-coated magnetic beads was tested via

fluorescence-based binding assays using SELEX conditions (Figure S1A). Five concentrations, ranging from 0 to 600 nM , of each fluorescein-labeled aptamer were incubated in $200\text{ }\mu\text{L}$ of BB at $90\text{ }^\circ\text{C}$ for 10 min, immediately cooled on ice for 15 min, and then incubated at RT for 3 min for thermal equilibration. These prepared solutions were incubated with a constant amount (9×10^7) of washed target-coated magnetic beads for 30 min at RT, with shaking. The unbound aptamers were then removed by two rigorous washing steps with $200\text{ }\mu\text{L}$ of BB, each. The bound aptamers were eluted twice by incubation of the aptamer–target complex, once with $200\text{ }\mu\text{L}$ of BB at $95\text{ }^\circ\text{C}$ for 9 min and once with $200\text{ }\mu\text{L}$ of EB at $80\text{ }^\circ\text{C}$ for 7 min, with shaking. The eluted DNA was determined by fluorometry (SPECTRAMax GEMINI, Molecular Devices, Belgium) using excitation and emission wavelengths of 485 and 535 nm, respectively. The sample volume was $180\text{ }\mu\text{L}$ /well in 96-well flat-bottomed black microtiter plates (Greiner bio-one, Belgium). The ssDNA concentrations were calculated by using calibration plots, and based on these data, saturation curves were obtained by plotting the amount of eluted aptamer versus the amount of total incubated aptamer. The K_d was calculated by fitting the data points by the nonlinear regression analysis with the help of the following equation, $y = B_{\text{max}} \times x / (K_d + x)$, using GraphPad Prism software.

As references, assays were performed exactly as described here but with quenched ethanolamine-coated magnetic beads instead of PCB-coated beads, in order to check for aspecific binding to the beads matrix. On the basis of those data, binding curves were obtained for each of the three aptamers to the reference beads as well, in order to be compared to the binding curves derived from the PCB-coated beads.

Relative Affinity Tests of Individual Aptamers via Indirect Competition Assays.

Based on the saturation binding assays, the two most promising aptamers were tested for their capability to bind to the free (not immobilized) targets, OH-PCB72 and OH-PCB106. They were further tested for their recognition abilities to some dioxin-like PCBs such as PCB105, PCB118, and PCB169 and a nondioxin-like PCB153 via indirect competition assays (Figure S1B). Roughly, $200\text{ }\mu\text{L}$ solutions of each fluorescein-labeled aptamer (700 nM) were denatured and renatured in BB, as explained earlier. These prepared solutions of each aptamer were then incubated with each of the six PCBs ($4.5\text{ }\mu\text{M}$ final concentration), in individual assays, and allowed to interact for 30 min. The mix containing the PCB–aptamer complex, free PCB, and free aptamer was then shaken with a constant amount (9×10^7) of washed PCB-coated magnetic beads for 30 min at RT. Using a magnet, the beads were drawn to a side of the vial, and the supernatant was gently removed in order to be measured. This supernatant would contain the free respective PCB along with the proportion of aptamer that bound to the free PCB rather than to the PCB-coated magnetic beads; hence, this was a competition assay where the aptamer was made to bind to free PCBs (OH-PCB 72 and 106 and PCB 105, 118, 153, and 169) (Figure 2) versus the OH-PCB bound beads. The DNA in the supernatant was determined by fluorometry and recorded as relative fluorescence units (RFU). As reference assays, no free PCB was added to the aptamer solutions, in order to take account of the aptamers that remained free in solution even when no free PCB was added, as there is always an equilibrium state where a part of the aptamers remains unbound. Individual reference assays were conducted for each PCB sample. Using these data, ratios were obtained of the RFUs in the PCB

samples to the RFUs in the reference samples. Ratios >1 imply that more aptamers remain in the solution of the PCB assay than in the reference assay, indicating an affinity of the aptamer for that respective PCB that is free in solution; the higher the value of the ratio, the higher the affinity of the aptamer for that specific congener. Ratios <1 imply lesser aptamers remaining free in solution of the PCB assay than the reference assay because of the possibility of the aptamer adopting a more active conformation after incubation with the free PCBs and thereby having greater binding toward the coated beads than in the reference assay. This test enables determination of the aptamer's ability to bind free PCBs and also provides an index to compare the relative affinity of the selected aptamers for each of the free PCBs tested.

RESULTS

Immobilization and Characterization of OH-PCBs (72 and 106) onto Magnetic Beads. The OH-PCBs had been coupled onto COOH-conjugated magnetic beads after activating the beads with carbodiimide and following an overnight incubation in 37 °C. The coating process is the binding of the COOH groups on the surface of the magnetic beads with the hydroxyl groups on the PCBs (Figure 2). The coupling procedure was directly analyzed by IR spectroscopy. Figure 3 illustrates that the spectrum of the OH-PCB-coated

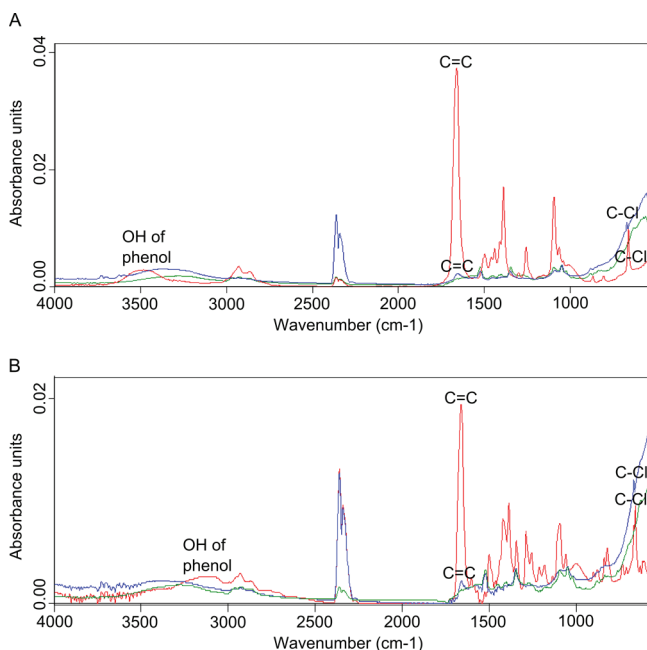


Figure 3. Infrared spectra of (A) OH-PCB72 (red), OH-PCB72-coated magnetic beads (blue), and ethanolamine-coated magnetic beads (green); (B) OH-PCB106 (red), OH-PCB106-coated magnetic beads (blue), and ethanolamine-coated magnetic beads (green).

beads is a merger of the OH-PCB spectrum and of the ethanolamine-coated beads spectrum. This signifies that the key characteristics of both, the beads and the PCBs, were present on the OH-PCB-coated beads, denoting a successful reaction which preserves the main features of the two reagents.

In Vitro Selection of PCB-Binding Aptamers for PCB72 and PCB106. Aptamers were isolated from a random ssDNA library by the SELEX process (Figure 1) using COOH-conjugated magnetic beads as the immobilization matrix for the

two PCB targets. The selected oligonucleotides of round eight of each of the two PCBs were incubated with the other PCB-coated beads for the final selection round, in order to isolate common aptamers that could recognize both the target PCBs and thereby a more common PCB skeleton. These were then amplified by PCR using unmodified primers to enable cloning of the aptamer pool. Three potential clones that carried aptamer fragments, namely 9.1, 9.2, and 9.3, were subjected to analysis and characterization. Aptamers 9.1 and 9.2 were common to both the pools whereas aptamer 9.3 was only present in the pool that was selected against PCB72 (following one selection round against PCB106). Their hypothetical secondary structure models were predicted by the Zuker algorithm (Figure 4A), and the variable N40 sequence regions of the aptamer candidates were aligned using GENEDOC software (Figure 4B). All sequences appeared to be distinct. Secondary structural prediction did not reveal any global structural similarities among the selected aptamers which all consisted of different stem and loop models. Similarly, there was no single consensus sequence that is conserved among the sequenced clones. The computed similarities of the conserved nucleotides (21st position \rightarrow T; 28th position \rightarrow C; 34th position \rightarrow C) are shown in Figure 4B, and their positions are boxed in Figure 4A. All of the clone sequences revealed a strong tendency toward C-richness ($>25\%$) with 9.1, 9.2, and 9.3 containing 36.25%, 32.5%, and 38.75% of cytosine residues, respectively (Figure 4B).

Saturation Binding Assays and Determination of K_d of Individual Aptamers. Saturation binding assays for the determination of dissociation constants of the individual aptamers to their two target PCBs were carried out by performing fluorescence-based affinity assays (Figure S1A, Supporting Information). Binding curves plotting the measured amount of bead-bound aptamers versus the corresponding input-aptamer concentration used are presented in Figure 5. The three sequences displayed notable differences in their relative binding capacities toward each of the three sets of beads (OH-PCB72-coated beads, OH-PCB106-coated beads, and quenched ethanolamine beads). Aptamer 9.3 showed the highest affinity for both the PCB structures present on the beads, with K_d values in the low nanomolar range of ~ 60 to 100 nM (Figure 5). This aptamer also displayed the lowest nonspecific binding to the background which is represented by its low binding curve toward the quenched ethanolamine beads. The K_d values for aptamers 9.1 and 9.2 were comparatively higher, and they also displayed increased binding toward the beads matrix.

Binding of Aptamers to Free PCBs and Relative Affinity Tests of the Aptamers. The aptamers in this study were selected for binding to immobilized PCBs on magnetic beads. The two highest binding aptamers were further characterized for their ability to bind to free PCBs (OH-PCB72 and OH-PCB106) in solution, as targets that were not immobilized. Moreover, the universality of the aptamers was tested by investigating if they could recognize other PCB congeners such as PCB105, PCB118, and PCB169 which are dioxin-like PCBs and a nondioxin-like PCB153. These goals were achieved via indirect competition assays (Figure S1B). The aptamers were first made to interact with each of the six PCBs in individual assays, and then the mix was introduced to the original PCB-coated beads, thereby creating a competition between the immobilized PCB (i.e., what they were originally selected for) and free PCBs (i.e., the form in which a PCB

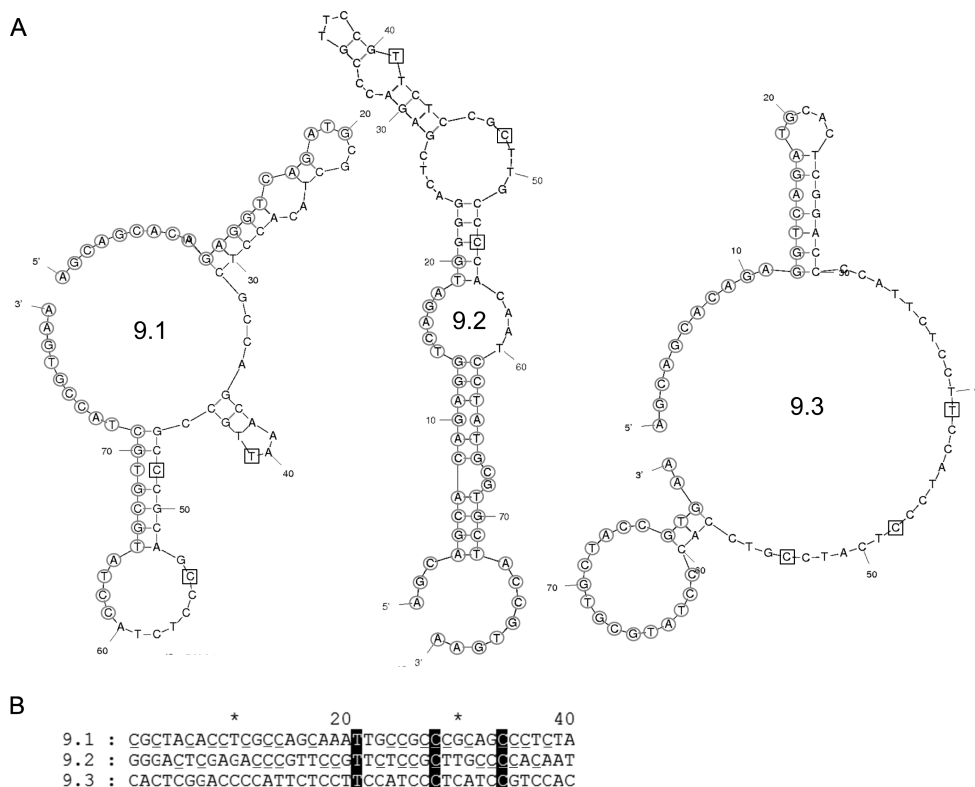


Figure 4. Analysis of the three aptamer sequences. (A) Predicted secondary structures of clones 9.1, 9.2, and 9.3 as determined by the *mfold* tool. The nucleotides involved in the primer regions (nucleotides 1–20 and 61–80) are marked by circles, and the conserved nucleotides are enclosed in boxes. (B) Sequence alignments of the aptamer random regions in 80-mer aptamers flanked on both sides by 20 nucleotide constant regions (5'-AGCAGCACAGAGGTCAGATG-N40-CCTATGCGTGCTACCGTGAA-3'). The conserved nucleotides are shaded in black representing those nucleotides found in all three sequences at the same position. The cytosine residues are underlined to emphasize the high-C content of the sequences.

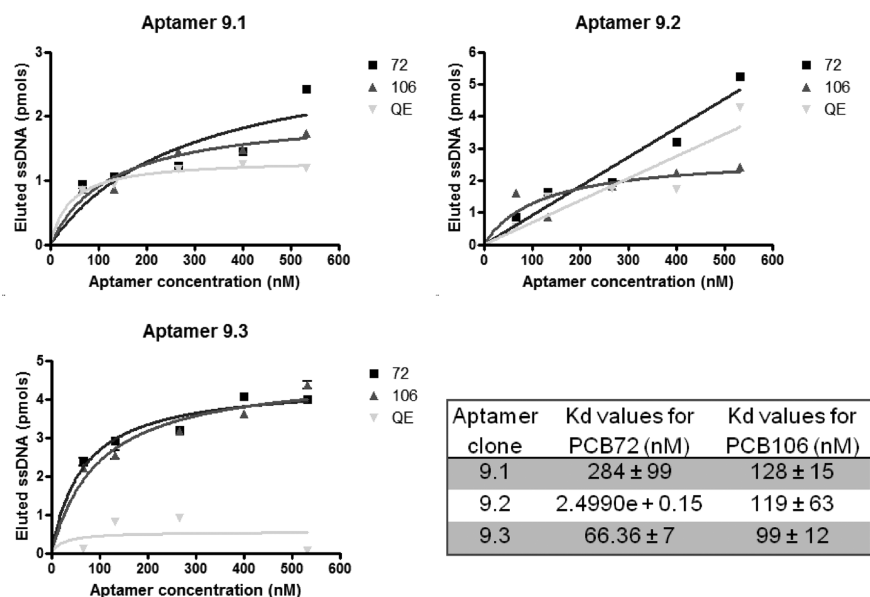


Figure 5. Saturation curves of aptamers 9.1, 9.2, and 9.3 to OH-PCB72 (72)-coated magnetic beads, OH-PCB106 (106)-coated magnetic beads and quenched ethanolamine (QE) magnetic beads. Data is presented as mean ± SD, $n = 3$ measurements of the same sample. The estimated K_d values of the aptamers are indicated in the bottom right corner.

would most likely be present in real-life samples). Figure 6 compares the relative affinity of the aptamers for each of the PCBs, which is the ratio of the RFU of the aptamer in the individual PCB assay to that of the reference assay. Aptamer 9.1

had all ratio values <1 which indicate its strong affinity toward the coated beads rather than to the free PCBs. Therefore, this aptamer will not be considered for further analysis or application. However, aptamer 9.3 revealed all ratios >1.

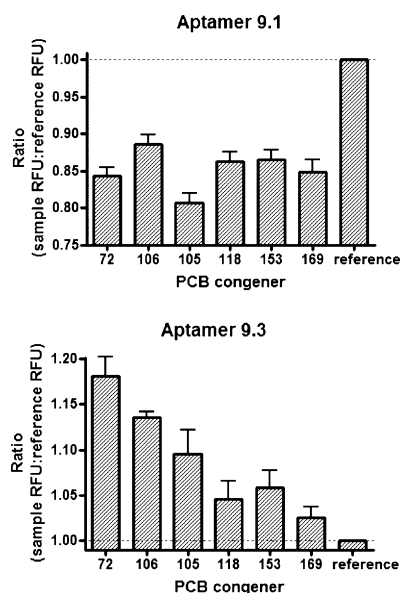


Figure 6. Indirect competition assays with aptamers 9.1 and 9.3 to investigate the ability of these aptamers to recognize free OH-PCB72 (72), free OH-PCB106 (106), free PCB105 (105), free PCB118 (118), free PCB153 (153), and free PCB169 (169). The bound aptamer to the respective free PCB was measured in relative fluorescence units (RFU). As references, similar assays with no added PCB were performed. On the basis of these data, ratios were obtained of the PCB samples RFU to the reference samples RFU. These ratios provide a relative index to compare the affinity of the selected aptamers for each of the six free PCBs. Data is presented as mean \pm SD, $n = 3$ measurements of the same sample, in a column graph format.

Overall, this aptamer had a higher affinity for the PCBs for which it was originally selected, though it could also recognize other congeners with limited affinity.

DISCUSSION AND CONCLUSIONS

This study describes the characterization of an aptamer that can bind with high affinity and specificity to PCBs. To our knowledge, this denotes the first study chronicling aptamer development for any of the POPs. The first step of the SELEX procedure for low molecular weight compounds is to immobilize them firmly onto solid supports.²⁶ For small molecules, such as PCBs, specific functionalizations are essential to facilitate their immobilization. Fixing the PCB onto a solid support was a nontrivial step, as the problem of lack of reactivity of PCBs had to be bypassed and the availability of functionalized PCBs is rather limited. Ultimately, two PCB congeners, 72 and 106, were immobilized in their hydroxylated forms and used as targets for aptamer selection. This hydroxylation permits coupling the PCBs onto COOH-conjugated magnetic beads,²⁷ without changing their binding properties. The immobilization strategy that was used here is the direct immobilization by organic synthesis. By fixing the synthesized PCBs at the hydroxyl terminus and allowing the rest of the PCB to be free, the bound PCB should simulate a conformation that appears in natural matrixes. Following this, aptamers that effectively identified the parent PCB structure without the OH group could be isolated. The use of target-bound magnetic beads allows for efficient separation between bound and unbound aptamers in the affinity selection procedure²⁸ via the use of a magnetic stand. IR spectroscopy

was used for qualitative characterization of the compound coupling. The characteristic peaks of the OH-PCBs are clearly found in the spectrum of the coated beads (Figure 3): the stretching vibrations of the aromatic rings (C=C) at 1650 cm^{-1} and the stretching of C-Cl at 660 cm^{-1} . The multiple peaks of the aromatic ring occurring between 1300 to 1600 cm^{-1} seem to have reduced in height or to have shifted in the spectra of the beads. This shift and/or lower signal can be due to the flexibility of that part of the PCB on the bead being limited, as the bead is larger than the molecule on the order $\sim 10\,000$ fold and consequently results in shifted or smaller peaks.²⁹ Nevertheless, the presence of those peaks, even though at a lower impact, indicates no loss in structure but simply restricted movement. The wide peaks that are observed between 3100 and 3600 cm^{-1} on the beads are derived from polystyrene, the composite material of the beads. Another observation worth stating was that the peaks corresponding to the OH of the phenols at 3500 cm^{-1} and 3100 cm^{-1} for OH-PCB 72 and OH-PCB106, respectively, disappeared in the target-coated beads, indicating that the coupling occurs via this group. Overall, the active groups of the PCBs are represented on the respective PCB-coated beads, indicating no loss in structure or quality and reinforcing the strength of the coupling reaction. This ensures that the aptamers selected subsequently are specific to the target in its original form.

DNA aptamers specific for PCBs were selected from a library containing approximately 10^{15} ssDNA molecules. To avoid selecting oligonucleotides that have an affinity for the background (beads, vials, etc), a counter-selection step was incorporated prior to every affinity selection cycle. In this counter-selection, the ssDNA molecules which bind to beads quenched with ethanolamine were discarded. After nine rounds of selection, three different sequences that recognize both PCB targets were characterized. The absence of a global consensus in the aptamer sequences and lack of a common predominant predicted structural motif suggests that a variety of DNA structures can bind to PCBs under the selection conditions used. Since PCB is a multifaceted molecule, different sequences could recognize different sites. The primer regions were always contained in the stem-loop structures, indicating their importance in the aptamer's binding properties or, in any case, stabilizing the aptamer structure to enable binding (Figure 4A). A further investigation for the sequence-match among the three clones disclosed some conserved nucleotides which could be predicted to be binding sites. Overall, the selected aptamers in this study had variations in their sequences and thus had distinct structural features and binding affinities. These differences in binding capabilities can be associated with the impact of the distinctive stem and loop structures and hence the different binding modes. Aptamers 9.1 and 9.2 have higher binding toward the bead matrix (Figure 5) and hence were common to both pools because the beads perhaps play a major role in their recognition abilities and have an affinity for the PCB-bead complex rather than just the PCBs. The results suggest an association between C-rich sequences and an affinity for PCBs, with this tendency being specifically predominant in sequence 9.3 that binds the PCBs most tightly and selectively. This aptamer displayed high affinity for the PCB structures present on the beads, with apparent K_d values clustered in the range of 60–100 nM (Figure 5). These affinities correlate well with previous studies on aptamers targeting diverse small molecules, such as ethanolamine,²⁸ oxytetracycline,³⁰ and fumonisins B₁,³¹ which have K_d values ranging from 6 to 121

nM. It has been hypothesized that targets containing aromatic ring structures, such as PCBs, enable stable noncovalent interactions with nucleic acids³² such as aptamers and thereby nanomolar affinity is conceivable. Current sensor platforms have exhibited detection levels up to 10 pg/mL with submicromolar affinity aptamers,³³ implying that aptasensors can be promising in reaching the detection limits that are required for PCBs (≈ 500 nM) in food or environmental samples, as designated by authorities such as FDA and Environmental Protection Agency (EPA). Matrixes such as soil or crude food samples, which contain complex matrix elements and also many other contaminants that can hinder aptamer detection, might necessitate some sample preparation such as preconcentration or extraction steps.

To confirm that the aptamers were selected for the immobilized PCBs and not for the magnetic beads, which was the immobilization matrix during SELEX, the affinity of the aptamers for the beads was tested as well. The low amount of aptamer 9.3 that was eluted by the quenched beads proves that the aptamer was specific for the immobilized PCBs in comparison to the solid support. To further test the aptamer interactions with free PCBs, the aptamer was subjected to indirect competition assays with free PCBs such as the target PCB congeners and additional PCBs such as 105, 118, 153, and 169. The free PCBs in solution were found to considerably attract the aptamer during the affinity assays, suggesting good affinity between the aptamer and the unbound PCBs as well. This could be due to the aptamer's binding to a particular conformation of the PCB, which is also available on the immobilized PCB, even while the PCB is attached to a much bigger bead molecule. Aptamer 9.3 which displayed the best affinity for the PCB targets was found to display good recognition for its original targets, clearly distinguishing those congeners from the rest. It had the greatest affinity for the free OH-PCB72 followed by OH-PCB106. This is logical because the aptamer was isolated from the eighth round of the PCB72 selections which was then introduced to PCB106 in the ninth round. Therefore, its specificity toward OH-PCB106 was slightly reduced considering that it had been exposed to that PCB for just one round. The ratios of this aptamer for nontarget PCBs 118, 153, and 169 indicate some affinity for those PCBs as well but to a lesser extent. However, it displayed high affinity against nontarget PCB105, implying a possibility for cross-reactivity. This cross-recognition indicates the formation of aptamer–PCB complexes with PCB106 which are equally favorable to that of the PCB105 complex. This is expected because these two congeners differ in the position of just one chlorine; instead of the meta position in PCB106, it is in the para position for PCB105 (Figure 2). This suggests that the majority of the aptamer structure binds to the part common of both PCBs. Contrarily, the limited binding behavior shown toward PCB169 suggests the aptamer's low affinity toward PCBs that are not substituted at any of the ortho positions, since congener number 169 is the only one (out of the six) lacking a chlorine atom at an ortho position (Figure 2). This absence could have obstructed the aptamer binding to the PCB either through steric hindrance or by limiting the number of available binding sites. However, the fact that the aptamer shows binding, whether extensive or limited, toward all the tested PCBs, suggests that the aptamer exhibits specific affinity for the characteristic biphenyl structure in the PCB skeleton. This is valuable because biphenyl is the defining and common trait among the wide variety of toxic PCBs found in the

environment. For this reason, PCBs 72 and 106 consisting of chlorine substitutions in different positions were chosen as targets for aptamer selection, in order to get a more general PCB-recognizing aptamer. Overall, this aptamer had higher affinity for the PCBs for which it was originally selected (exhibiting the ability of aptamer technology to differentiate between targets as closely related as PCB congeners), though it could also recognize other congeners with limited affinity. Therefore, this aptamer can be seen as a general PCB-specific aptamer with varying affinities for different congeners and is specific for the PCB skeleton structure in its known form (i.e., as a free target). This is imperative because if the aptamers are further developed as recognition elements in sensors for detection of the target in food or environmental samples, the samples will contain the original form of the target. In conclusion, aptamer 9.3 which contains C-rich sections (38.75%), showed high affinity and increased binding toward the PCB targets and hence further convinces us of the implications of these structural elements.

The DNA aptamers that were isolated in this study are new alternatives of PCB-specific recognition molecules. The incorporation of PCB-specific aptamers in biosensors or detection assays should lead to improved functionality and reduced expense in monitoring of PCB-contaminated food and environmental samples. The identification of this sensitive and specific aptamer is the gateway to developing a robust, cost-effective sensor that will bridge the gap between environmental PCB exposure and clinical outcomes. Furthermore, by being able to potentially block the endocrine disrupting function of PCBs, such aptamers could even provide a foundation for therapeutics.³⁴ Overall, this study demonstrates the viability of producing aptamers for POPs using PCBs as targets and offers a platform for prospective future development of aptamers that target other POPs, thus paving the way for further environmental research and application.

■ ASSOCIATED CONTENT

Supporting Information

Additional information as noted in the text. This material is available free of charge via the Internet at <http://pubs.acs.org>.

■ AUTHOR INFORMATION

Corresponding Author

*Tel: +32-(0)3-265.35.41. Fax: +32-(0)3-265.34.97. E-mail: Jaytry.Mehta@ua.ac.be.

Present Address

#Companion Diagnostics COE, Tibotec-virco Virology, Turnhoutseweg 30, B-2340 Beerse.

■ ACKNOWLEDGMENTS

The authors thank Mandira Banerji for editorial assistance. This study was funded by the Federal Public Service of Health, Food Chain Safety and Environment (contract RT 07/11 INVI-TRAB).

■ REFERENCES

- (1) Nowak, K. *Elektrische Maschinen*/Elektrische Maschinen. **1986**, 65, 376–86.
- (2) Gedik, K.; Imamoglu, I. *Environ. Sci. Pollut. Res.* **2011**, 18, 968–977.
- (3) Jones, K. C.; de Voogt, P. *Environ. Pollut.* **1999**, 100, 209–221.
- (4) Liu, S. J.; Zhang, S. P.; Qu, C.; Liu, W.; Du, Y. G. *Sci. China-Chem.* **2010**, 53, 974–979.

- (5) Crinnion, W. J. *Altern. Med. Rev.* **2011**, *16*, 5–13.
- (6) Rocheleau, C. M.; Bertke, S. J.; Deddens, J. A.; Ruder, A. M.; Lawson, C. C.; Waters, M. A.; Hopf, N. B.; Riggs, M. A.; Whelan, E. A. *Environ. Health* **2011**, *10*, 20.
- (7) Srogi, K. *Environ. Chem. Lett.* **2008**, *6*, 1–28.
- (8) Brambilla, G.; Cherubini, G.; De Filippis, S.; Magliuolo, M.; di Domenico, A. *Anal. Chim. Acta* **2004**, *514*, 1–7.
- (9) Mydlova-Memersheimerova, J.; Tienpont, B.; David, F.; Krupcik, J.; Sandra, P. *J. Chromatogr., A* **2009**, *1216*, 6043–6062.
- (10) Glass, T. R.; Ohmura, N.; Morita, K.; Sasaki, K.; Saiki, H.; Takagi, Y.; Kataoka, C.; Ando, A. *Anal. Chem.* **2006**, *78*, 7240–7247.
- (11) Fang, X.; Tan, W. *Acc. Chem. Res.* **2009**, *43*, 48–57.
- (12) Ellington, A. D.; Szostak, J. W. *Nature* **1990**, *346*, 818–822.
- (13) Jianwei, X.; Jijun, T.; Tao, Y.; Lei, G.; Ningsheng, S.; Zhike, H. *Biosens. Bioelectron.* **2007**, *22*, 2456–63.
- (14) Van Dorst, B.; Mehta, J.; Bekaert, K.; Rouah-Martin, E.; De Coen, W.; Dubruel, P.; Blust, R.; Robbens, J. *Biosens. Bioelectron.* **2010**, *26*, 1178–1194.
- (15) Low, S. Y.; Hill, J. E.; Peccia, J. *Biochem. Biophys. Res. Commun.* **2009**, *378*, 701–705.
- (16) Kim, Y. S.; Jung, H. S.; Matsuura, T.; Lee, H. Y.; Kawai, T.; Gu, M. B. *Biosens. Bioelectron.* **2007**, *22*, 2525–2531.
- (17) Kim, Y. J.; Kim, Y. S.; Niazi, J. H.; Gu, M. B. *Bioprocess Biosyst. Eng.* **2010**, *33*, 31–37.
- (18) Wei, F.; Ho, C. M. *Anal. Bioanal. Chem.* **2009**, *393*, 1943–1948.
- (19) Bruno, J. G.; Kiel, J. L. *Biotechniques*. **2002**, *32*, 178–+.
- (20) Ding, S.; Gao, C. L.; Gu, L. Q. *Anal. Chem.* **2009**, *81*, 6649–6655.
- (21) Hua, K.; Wei, C.; Dinghua, X.; Liguang, X.; Yingyue, Z.; Liqiang, L.; Huaqin, C.; Chifang, P.; Chuanlai, X.; Shuifang, Z. *Biosens. Bioelectron.* **2010**, *25*, 710–16.
- (22) Tuerk, C.; Gold, L. *Science* **1990**, *249*, 505–510.
- (23) Mendonsa, S. D.; Bowser, M. T. *Anal. Chem.* **2004**, *76*, 5387–5392.
- (24) Mehta, J.; Van Dorst, B.; Rouah-Martin, E.; Herrebout, W.; Scippo, M.-L.; Blust, R.; Robbens, J. *J. Biotechnol.* **2011**, *155*, 361–369.
- (25) Zuker, M. *Nucleic Acids Res.* **2003**, *31*, 3406–3415.
- (26) Codrea, V.; Hayner, M.; Hall, B.; Jhaveri, S.; Ellington, A. *Current Protocols in Nucleic Acid Chemistry*; John Wiley & Sons, Inc.: New York, 2001.
- (27) Shelkov, R.; Nahmany, M.; Melman, A. *Org. Biomol. Chem.* **2004**, *2*, 397–401.
- (28) Mann, D.; Reinemann, C.; Stoltenburg, R.; Strehlitz, B. *Biochem. Biophys. Res. Commun.* **2005**, *338*, 1928–1934.
- (29) Mondal, S.; Hu, J. L. *Polym. Eng. Sci.* **2008**, *48*, 233–239.
- (30) Niazi, J. H.; Lee, S. J.; Kim, Y. S.; Gu, M. B. *Bioorg. Med. Chem.* **2008**, *16*, 1254–1261.
- (31) McKeague, M.; Bradley, C. R.; Girolamo, A. D.; Visconti, A.; Miller, J. D.; DeRosa, M. C. *Int. J. Mol. Sci.* **2010**, *11*, 4864–4881.
- (32) Yang, Q.; Goldstein, I. J.; Mei, H. Y.; Engelke, D. R. *Proc. Natl. Acad. Sci. U.S.A.* **1998**, *95*, 5462–5467.
- (33) Hansen, J. A.; Wang, J.; Kawde, A. N.; Xiang, Y.; Gothelf, K. V.; Collins, G. *J. Am. Chem. Soc.* **2006**, *128*, 2228–2229.
- (34) Ditzler, M. A.; Bose, D.; Shkriabai, N.; Marchand, B.; Sarafianos, S. G.; Kvaratskhelia, M.; Burke, D. H. *Nucleic Acids Res.* **2011**, *39*, 8237–8247.